# LINEWIDTH MEASUREMENTS OF FLUX-FLOW JOSEPHSON OSCILLATORS USING A CAD DESIGNED INTEGRATED SUB-MM WAVE RECEIVER

Y.M. Zhang, D. Winkler, and T. Claeson
Department of Physics
Chalmers University of Technology
S-412 96 Göteborg, SWEDEN

## ABSTRACT

By using a superconducting integrated sub-mm wave receiver, the linewidth of a flux-flow type Josephson oscillator (FFO) was measured to be less than 2.1 MHz in the band 280–330 GHz. The output power coupled to a 10 Ω microstripline was about 0.5 μW, and could be adjusted by changing the current bias of the oscillator junction.

The integrated receiver consists of two identical Josephson flux-flow oscillators and an SIS (superconductor-insulator-superconductor) mixer. We can determine the composite linewidth of the oscillators by mixing them down to an intermediate frequency in the SIS mixer. The FFOs are connected to the SIS mixer via centerfed interdigital capacitors. One FFO is well coupled to the SIS mixer by using a 3-step Chebychev microstripline transformer and a fairly large interdigital capacitor, while the second FFO has about 15 - 20 dB weaker coupling. A strip inductor, *rf*-terminated by a radial stub resonates out the SIS junction capacitance at about 340 GHz. Radial stubs were also used as RF chokes for the *if*-line (4 GHz). The FFOs and the SIS element are made of Nb/Nb-oxide/PbBi tunnel junctions.

The circuit was optimized by careful CAD modeling (HP Microwave Design System). Normal conductors were used with the resistivity set to zero. Microstripline widths and lengths were recalculated for the superconducting case with the London penetration depths of the electrodes (Nb and PbBi) taken into account. After adjusting the area of the SIS element and the length of the tuning strip inductor, a good response was observed from 280 to 330 GHz, with the LC resonance at 340 GHz. The power was high enough to pump the SIS mixer.

## 1. INTRODUCTION

For space born missions, low weight and small volume are required. When it comes to imaging arrays, this is even more of a concern. By using SIS (superconductor-insulator-superconductor) mixers with much less local oscillator (LO) power requirements some of the problems can be alleviated. Even better would be if the external LO could be replaced with an on-chip fully integrated source. The concept of using superconducting technology for the construction of low-noise, integrated millimeter or submillimeter-wave receivers has been considered as a promising idea for many years. However, not until recently has sufficient progress been made to

really demonstrate the possibilities. One way to achieve practical oscillators is by using coherent, mutually phase-locking arrays. Bi *et al.* [1] measured a 10 MHz linewidth by mixing two Josephson array oscillators at 250 GHz. Sufficient available power existed to pump an SIS mixer, but the number of junctions in the oscillator or the coupling strength to the SIS mixer had to be fixed at the design stage to obtain the optimum local oscillator power for the design frequency .

Another way to achieve a practical oscillator is by using the fluxon (flux quantum $\Phi_0=h/2e$) propagation in a long Josephson tunnel junction (LJJ), either in a resonant mode (back and forth propagation of solitons) or in a unidirectional flux-flow mode. A soliton (fluxon) is an electromagnetic pulse and gives rise to the emission of a pulse of electromagnetic energy when it hits the end of the junction. If the arrival of solitons at one end of the junction is periodic, *rf* radiation is emitted. The propagation mode of the fluxon in a LJJ depends on the junction quality factor $Q_J$, which is related to the junction losses as [2]

$$Q_J = ((\omega_0/\omega_J)^2 \beta + \alpha)^{-1} \quad , \qquad (1)$$

where $\omega_0=(2\pi/\Phi_0)V_{dc}$ is the frequency of Josephson oscillation ($V_{dc}$ is the dc voltage of the junction, $\omega_J$ is the Josephson plasma frequency, $\beta$ is the surface loss, and $\alpha$ is the quasiparticle loss).

*The first type of fluxon oscillator* is called resonant soliton oscillator (RSO), which uses a long junction with a high quality factor $Q_J$ (low quasiparticle loss $\alpha$). In order to achieve a high $Q_J$, the junction should have a low critical current density $j_c$ [3]. Driven by the bias current, a fluxon travels along the junction until it reaches the junction boundary, where it is reflected as an anti-fluxon, which in turn is driven in the opposite direction. This process is repeated, resulting in a microwave emission at a frequency given by [4]

$$f = V_{dc} / 2\Phi_0 = nu / 2L \quad , \qquad (2)$$

where $u$ is the average fluxon velocity, n is the number of fluxons moving in the junction of length $L$. A RSO is operated at zero or a relatively weak external magnetic field. Its oscillation frequency is determined mainly by the junction length $L$ rather than the applied field and bias

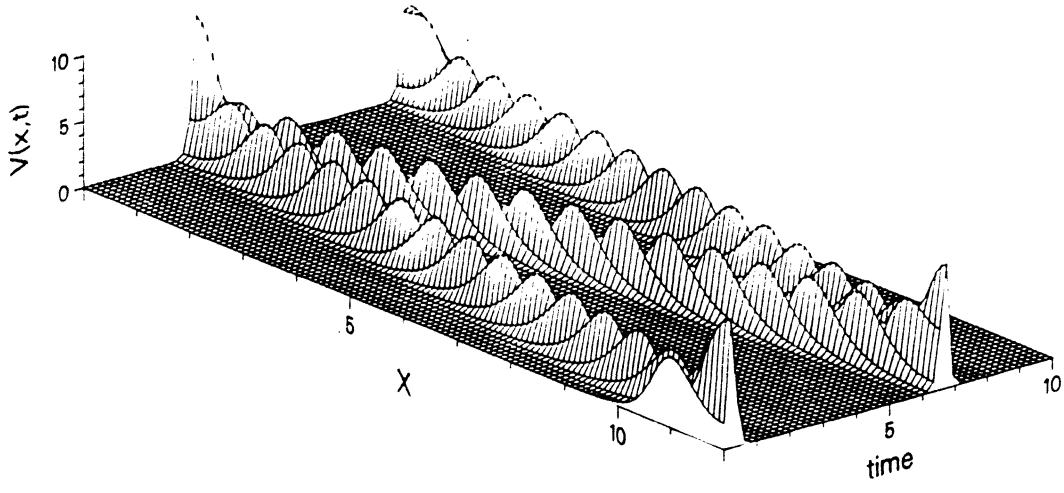


**Fig.1** Computer simulation showing time-dependent junction voltage V(x,t) of a LJJ in the single resonant soliton (n=1) case for parameters: $L/\lambda_J=12$, $\alpha=0.05$, $\beta=0.02$, $\gamma=0.35$ (at zero magnetic field).

current. This suggests a rather well defined frequency. The resulting resonant step in the characteristic is commonly called a zero field step (ZFS). When the oscillator is biased on a zero field step, the emitted radiation is characterized by a very narrow output linewidth - about 1 kHz at 10 GHz [5]. A main weakness of this kind of oscillators is its low output power - reported powers coupled to SIS detectors are less than 10 nW at ~100 GHz [6]. However, Cirillo *et al.*[7] have estimated a power of ~100 nW at 75 GHz into a tightly coupled small junction. The low output power is partially due to the low $j_c$ requirement for a RSO. Also, the output voltage waveform of a RSO consists of fairly sharp spikes, which suggests that the output power is delivered into a broad range of harmonics rather than being concentrated at the fundamental frequency. In Fig.1, we show a computer simulation for the single soliton propagation in a LJJ with overlap geometry. Note that this figure is in normalized units: distance x is normalized to the Josephson penetration depth $\lambda_J$, time is normalized to the inverse of $\omega_J$, and $\gamma$ is the bias current $I_B$ normalized to the maximum zero-voltage Josephson current $I_c$. Another weakness of a RSO is its upper oscillation frequency limited by the junction length $L$ which should be much larger than the Josephson penetration depth $\lambda_J$. This makes it difficult to operate at sub-mm wavelengths.

*The second type of fluxon oscillator* is called flux-flow Josephson oscillator (FFO). It is based on a long Josephson junction working in the viscous unidirectional flux-flow regime. In order to maintain fluxons moving unidirectionally under the Lorentz force, a dc magnetic field $H_e$ is applied in the plane of the junction, and the junction should have a low quality factor $Q_J$ (high quasiparticle loss $\alpha$). This means a high $j_c$ value is necessary for an FFO [6]. When the velocity of the flux-flow $u$ approaches that of the electromagnetic wave $\bar{c}$ propagating along a LJJ, a resonant like current step appears in the I-V characteristic. This resulting step is commonly called velocity-matching step (VMS). A computer simulation illustrating flux-flow in a LJJ with overlap geometry is shown in Fig.2. The oscillation frequency can be tuned over a wide range by changing the applied field

$$f = V_{dc}/\Phi_0 = ud\mu_0 H_e/\Phi_0 \quad . \qquad (3)$$

Here, $d$ is the effective magnetic thickness of the junction barrier and $\mu_0$ is the permeability of free space. The FFO was early investigated both experimentally and by computer modeling by Nagatsuma *et al.* [2,8,9] and Zhang and Wu [10]. Relatively large output power in the sub millimeter wave band was obtained for this type of oscillator, e.g., powers of about 1 μW (into a small junction detector) up to 400 GHz was reported early [8], and power of about 0.5 μW coupled to a 10 Ω microstripline at 280 - 330 GHz was recently reported [11]. The high output power of an FFO is due to two reasons: i) high current density leads to a high bias current; ii) fluxons reach the output end in a tightly packed unidirectional train, thus the output voltage waveform is nearly sinusoidal, which suggests the output power is largely concentrated at the fundamental frequency. In principle, there is no limitation to the operation frequency of this kind of oscillator up to the energy gap of the superconducting electrode. However, there were serious doubts about its usefulness since no linewidth measurements had been done until recently. Its oscillation frequency, which relates to the vortex density inside the junction, depends strongly on the value of the external magnetic field. This means there exists another source of fluctuations that might broaden the output spectral linewidth. Ustinov *et al.* [12] have measured a linewidth of 120 kHz of an FFO working at 76 GHz. Koshelets *et al.* [13] have used an FFO integrated with an SIS mixer. They mixed the signal of a backward wave oscillator with the LO signal produced by the FFO in the SIS element, and measured an upper value of the linewidth to be about 1 MHz in the band 82 - 112 GHz.

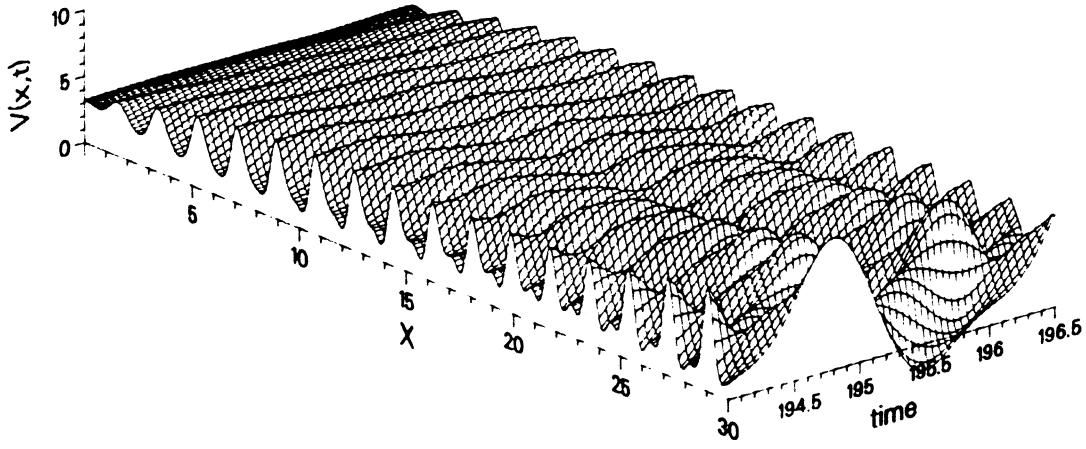


**Fig.2** Computer simulation showing time-dependent junction voltage V(x,t) of a LJJ in the flux-flow regime for parameters: $L/\lambda_J=30$, $\alpha=0.25$, $\beta=0.001$, $\gamma=1.015$ (in normalized units and at normalized magnetic field $\beta e$ [10]).

In this paper, we report the design of an integrated receiver in which we mix the output oscillations from two identical fluxon oscillators in a small SIS mixer and determine the linewidth of the oscillators from the intermediate frequency (*if*) with a spectrum analyzer. The circuit was optimized by using CAD modeling. We also show that a long-junction oscillator could be operated in either the resonant propagation mode or the flux-flow mode, depending on the critical current density of the oscillator junction.

## 2. DESIGN

To avoid problems of coupling mm- and sub-mm waves between different wave guide systems, and to be able investigate a variety of frequencies, we decided to make a fully integrated receiver where the output signals (local oscillator $f_{LO}$ and a weaker signal $f_S$) of two fluxon oscillators are mixed in an SIS element to a lower intermediate frequency ( $f_{if}=|f_{LO}-f_S|$ ). In this way, the two fluxon oscillators and the SIS mixer could be (i) fabricated all on the same chip, (ii) coupled by microstripline circuitry, and (iii) analyzed using only one coaxial line and dc-bias leads.

The circuit, which was designed to operate around 350 GHz, is outlined in Fig.3. Before describing the *rf* design of the total circuit and the CAD modeling, we will first examine the requirements on the fluxon oscillators and the SIS mixer.

### 2.1 Oscillators

In Fig.4, we show a SEM photograph for a receiver circuit. The long Josephson junctions (LJJ) are constructed in an overlap geometry with a length $L=400\mu m$ ($>>\lambda_J$). The bias current $I_B$ is applied perpendicular to the long dimension of the junction. In order to reduce the self field at the end where vortices are nucleated, a projection length of $50\mu m$ is employed (e.g., see left end of FFO1 in Fig.4). The characteristic impedance of a LJJ of width $w$ is given by

$$Z_o = \frac{120\pi}{w\sqrt{\varepsilon_r}}\sqrt{t\,d} \qquad (4)$$

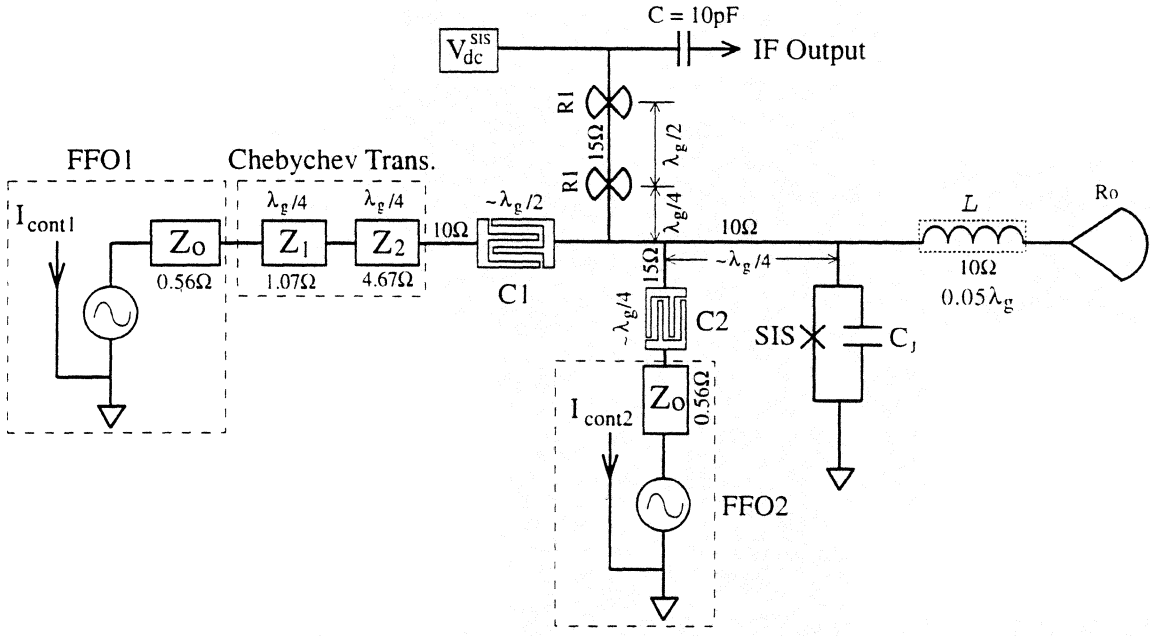


**Fig.3** The modeling circuit for measuring the linewidth of FFOs. By mixing two similar FFOs in the SIS element, we can determine the combine linewidth of the FFOs from the *if* product. FFO1 is used as a local oscillator, while FFO2 serves as the signal source.

For Nb/NbOx/PbBi junctions, the dielectric constant of the junction barrier ($Nb_2O_5$) $\varepsilon_r = 29$, the barrier thickness t ≈2 nm, and the magnetic thickness $d=t+\lambda_{Nb}+\lambda_{PbBi} \approx 287$nm. In order to match the output impedance $Z_o$ of the oscillator to the load, and to avoid resonant modes along the small dimension of the junction, we choose a narrow width ($w=3$ μm) for the LJJs ($Z_o=0.56\,\Omega$).

The junction critical current density, $j_c$, is an important fabrication parameter that controls the operation mode of a LJJ. We have shown that a long-junction oscillator could be operated in either the resonant propagation mode or the flux-flow mode, depending on the junction current density [6]. Here, we give a rough estimate of the lowest $j_c$ value for the flux flow mode. For simplicity, we use the junction normal state resistance $R_n$ instead of the dynamic resistance $R_d$ of the quasiparticle current at $V=V_{dc}$. Thus, the quasiparticle loss α can be written as [3]

$$\alpha = \frac{1}{I_c R_n}\sqrt{\frac{j_c \Phi_o}{2\pi C}} \quad , \tag{5}$$

where $C$ is the junction capacitance per unit area. The Josephson penetration depth $\lambda_J$ is given by

$$\lambda_J = \sqrt{\frac{\Phi_o}{2\pi\mu_o j_c d}} \quad . \tag{6}$$

Combining Eq.(4) and (6) together, we get

$$\alpha L/\lambda_J = \frac{j_c L w Z_o}{I_c R_n} \quad . \tag{7}$$

The condition for supporting the unidirectional flux-flow is $\alpha L/\lambda_J \geq 2$. Taking the typical value for Nb/NbOx/PbBi junctions $I_cR_n = 1.8$mV, we get $j_c \geq 540$ A/cm$^2$ ($L=400$μm, $w=3$μm,

$Z_o = 0.56\Omega$). Actually $j_c$ of an FFO should be at least 2 times higher than this value, because the dynamic resistance $R_d$ is usually a few times higher than $R_n$.

The external magnetic field to sustain the flux motion in a LJJ can be provided by injecting *dc* current through the base electrodes or through a separate control line (another Nb layer) under the LJJs. Two separate local fields were applied to FFO1 and FFO2 (as indicated by $I_{cont1}$ and $I_{cont2}$ in Fig.3). For obtaining a uniform distribution of bias current along the LJJ, we used multi-finger bias leads for both base and top electrodes (see Fig.4).

2.2 SIS detector

The SIS element should be well matched to the LJJ. A small junction area (i.e. small capacitance) is needed to get a reasonably large value of the tuning inductance for resonating out the junction capacitance at 340GHz. The junction capacitance $C_J$ is inductively compensated by a strip inductance $L$ and *rf* terminated by a radial stub $R_o$. The outer radius $r_2$ of the radial stub was calculated approximately from [14]

$$r_2 - r_1 = \lambda_g / 2\pi \quad , \tag{8}$$

where the inner radius $r_1$ was taken as the half width of the 10 Ω microstripline ($\lambda_g$ is the wavelength in the microstripline). The width of the 10 Ω microstripline is 6.9 μm for the superconducting case and 5.4 μm for the normal conductor. The outer radius was then optimized by the CAD simulation and recalculated for the superconductor case ($r_2$=35.2 μm).

The LC resonance frequency, given by $f_o = 1/2\pi\sqrt{LC_J}$, is very sensitive to the length of the strip inductance and the area of the SIS junction. Fortunately, the resonance frequency could usually be determined from the I-V curve of the SIS mixer, which had an additional step structure at the corresponding Josephson frequency ($f_o = 2eV/h$). From the LC resonance and by measuring the actual junction area in an SEM, we could get a fairly good control of the tuning of the SIS mixer for the second batch of samples that was fabricated. We varied junction sizes from 0.5 $\mu m^2$ to 4 $\mu m^2$ for different chips. The inductance length is 13.5 μm long for a junction size of 0.65 $\mu m^2$. For a 4$\mu m^2$ large junction, the inductor length would only be 2.2 μm long, which should be compared to the junction width and the microstripline width of 6.9 μm. Hence, the actual dimensions of the inductance is very critical. To avoid this difficulty, we have also made circuits, where two (about twice as long) inductors with separate radial stubs have been connected in parallel with the SIS element. The bandwidth of the SIS mixer around LC resonant frequency $f_o$ is given by

$$\frac{\Delta f}{f_o} = \frac{1}{\omega_o R_n C_J} = \frac{j_c}{\omega_o (I_c R_n) C} \quad . \tag{9}$$

Thus, the available bandwidth of the mixer is not dependent on the junction area, but depends on its $j_c$ value [15,16]. Knowing for Nb/NbOx/PbBi junctions, $I_c R_n = 1.8$mV, $C = 140$ fF/$\mu m^2$, we acquire $\Delta f = 6.3$ GHz for $j_c$=1 kA/$cm^2$. By increasing $j_c$ ten times to 10 kA/$cm^2$, we can have a quite wide bandwidth of 63 GHz. This indicates the importance of having a high $j_c$ SIS junction for a broad band response. Since both FFOs and the SIS junction on a chip were made within the same process steps, they had almost the same $j_c$ value. This means that for a LJJ working in the resonant mode, the response band for an SIS detector on the same chip is very narrow because of low $j_c$. That is why in experiments we found it was quite difficult to observe radiation from a low $j_c$ sample.

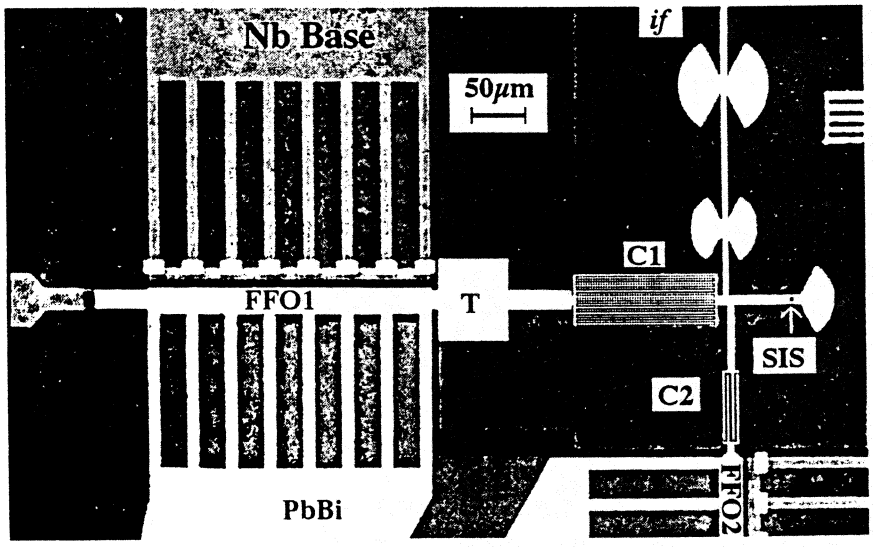


**Fig.4** SEM picture of the integrated receiver. The FFOs (3 μm wide by 350 μm long) are connected to an SIS mixer via centerfed interdigital capacitors (C1 and C2). T is the first section of the impedance transformer ($Z_1$ in Fig.3). The FFOs and the SIS element are made of Nb/Nb-oxide/PbBi tunnel junctions.

2.3 *rf* circuit

The *rf* performances of the circuit design was optimized by careful CAD modeling (HP 85150B Microwave Design System) with the center frequency at 350GHz. Normal conductors were used with the resistivity set to zero. Microstripline widths and lengths were recalculated for the superconducting case with the London penetration depths of the electrodes taken into account [17,18]. We take $\lambda_L$(Nb)=85 nm and $\lambda_L$(PbBi)=200 nm [19] for superconducting microstriplines Nb(200nm)/SiO(400nm)/PbBi(400nm) in the circuit. Also, we take $\varepsilon_r$ = 5.5 [20] for the SiO dielectric layer with the assumption that this holds also at 350 GHz.

Both oscillator junctions are connected to the SIS mixer via center-fed interdigital capacitors (see Fig. 3). These capacitors are necessary for separating the dc-biases of the FFOs and the SIS element. One oscillator (FFO1) is well coupled to the SIS mixer by using a 3-step Chebychev microstripline transformer and a fairly large interdigital capacitor C1 with 20 strips (see Fig.5 for detail). The center frequency of the Chebychev transformer [21] is 350 GHz, and its 3 dB bandwidth is 80 GHz. It transforms the low impedance of the oscillator $Z_0$ ( = 0.5 Ω) to the 10 Ω microstripline impedance through two λ/4 long microstriplines $Z_1$( = 1.07 Ω) and $Z_2$ (=4.67 Ω). The length of the finger coupler C1 has to be about λ/2 long rather than λ/4 to give sufficient coupling with available lithography. The problem is caused by the unfavorable small aspect ratio of the dielectric thickness (400 nm) and the strip separation (0.8 - 1 μm). CAD modeling showed that this capacitor could have 50 GHz bandwith (3 dB loss). The second FFO has about 15 - 20dB weaker coupling. It only contains four strips (63 μm long, 2 μm wide, and 2 μm as the gap). In this way the interaction between the two oscillators is fairly small. In Fig.5, we show the CAD modeled *rf* response of the circuit (for the normal conductor case). The transmitted power (S12) from the local oscillator (FFO1) to the SIS element has a bandwidth of 50 GHz. An additional window at around 100GHz, however with ~20 dB loss, is also seen in the calculation. Although this window is very narrow, we observe radiation from the oscillator to the SIS detector in this band.

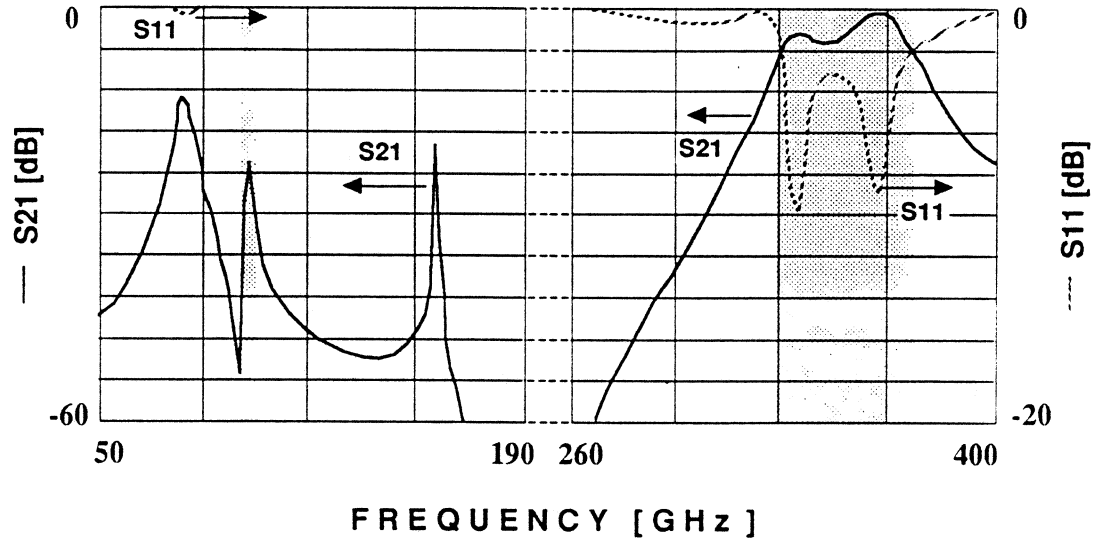


**Fig.5** *rf* characteristics of the modeling circuit. Microstriplines are based on lossless metals separated by a 400nm thick insulator layer with $\varepsilon_r$ of 5.5. S11 is the reflection from FFO1, S21 is the transmitted power from the FFO1 to the SIS element. We choose 10Ω for the resistance $R_n$ of the SIS mixer, and 560 fF for its capacitance $C_J$. Note that for the 260GHz response (see below), the actual circuit differed somewhat from this one.

The intermediate frequency (*if*) signal is transmitted through a 15 Ω microstripline (4 μm wide) filtered by two pairs of radial stubs (R1 in Fig.3). The radial stubs were used as *rf* chokes for the *if*-line. The outer radius of the radial stubs was calculated from Eq.(8), $r_2$=46.1 μm and $r_2'$=34 μm. The position of the *if*-line on the 10 Ω microstrip was optimized by CAD simulation (to minimize the effect of the *if*-line to the rf characteristics of the circuit). The 15 Ω microstripline was then transferred to a finline via a balun construction. One electrode of the finline (PbBi) is connected to a thin film capacitor (10pF), while the other is electrically connected to the Nb ground plane. The *if* characteristics of this circuit was simulated by CAD, and showed a flat transmission from the SIS element to IF output at the band around 4 GHz with a loss less than 1 dB. Before the thin film capacitor, the *if*-line also serves as the dc-bias line for the SIS mixer.

## 3. FABRICATION PROCEDURES

Low doped silicon wafers were used as substrates. About fifty 6 x 3.8 $mm^2$ chips of different designs were fabricated simultaneously, before dicing the wafer. The pattern of the last layer (PbBi) was defined by a direct electron beam writing for a single chip or a couple of chips at a time. This made adjustments of the circuit parameters very easy.

Both FFOs and the SIS element are fabricated by using Nb (200 nm) as base-electrodes, windows in SiO (400 nm) defining the junction areas, and PbBi (400 nm) as top-electrodes. First, a lift-off stencil for defining the Nb base electrodes is prepared with S1813 photoresist. Nb film is dc sputted at a rate of 0.5 nm/s. This Nb layer is also the ground plane for the microstriplines. Then, on top of the Nb patterns, another lift-off stencil for defining the Au contact pads is prepared. The Au layer is formed by thermal evaporation of 20 nm NiCr (0.1 nm/s) followed by 250 nm Au (1 nm/s). For a good contact between the Au and Nb layers,

Ar-ion beam etching is used just before the evaporation without breaking the vacuum to provide a fresh Nb surface.

Lift-off stencils for defining the junction windows in SiO as well as the top-electrodes are made by using electron-beam writing on PMMA/Copolymer double layer e-beam resist: copolymer (poly[methyl methacrylate/methacrylic acid] copolymer) 11% (650 nm) at the bottom and PMMA (poly[methyl methacrylate]) 3% (150 nm) on the top with an exposure dose of 220 $\mu C/cm^2$ at 50 kV. This high exposure dose works well for the lift-off process of the finger coupler which has 20 fingers (see Fig.6). SiO was thermally evaporated at a rate of 2.5 nm/s. The Nb/NbOx/PbBi tunnel junctions were formed by Ar-ion beam etching followed by reactive ion beam oxidation and a thermally evaporated PbBi (1nm/s) top electrode. The critical current density of the junction is controlled by the oxidation time and can be varied from 200 $A/cm^2$ to 20 $kA/cm^2$.

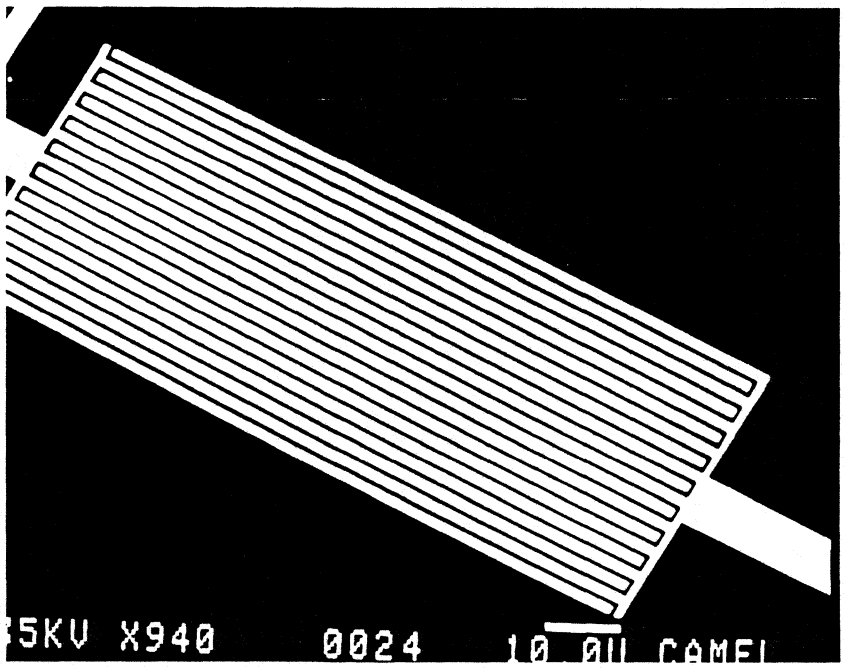


**Fig.6** SEM micrograph of a finger coupler (C1) made of 400nm PbBi. The coupler has 20 fingers (1.2μm wide, 180μm long and 0.8μm separation). It provides good rf-coupling and dc-block between FFO1 and the SIS element. Its length is about λ/2 long of the center frequency for the pass band. It is the most difficult part of this circuit, from the fabrication point of view.

## 4. EXPERIMENTAL

The integrated oscillators and SIS circuit was mounted in a 22 pin IC package. Gold pads on the chip were connected to the package by thermosonic wire bonding. The IC package was mounted onto an IC socket at the bottom of a closed-end dipstick (0.75 inch in diameter). Two pins on the IC socket are soldered to a UT85 coaxial cable (a 1nF chip capacitor on the outer jacket of the coax gives dc-isolation also on the ground side). Bias leads were filtered by low pass filters. The oscillators, SIS, and control currents were driven by stabilized battery sources. The chip package was shielded by Pb foil. The dipstick was immersed into a μ-metal shielded helium cryostat, and the measurements were done inside a screen room. The sample temperature could be adjusted from 4.2K to about 1K by pumping the liquid helium. The *if* signal was

transmitted through the coaxial line to room temperature *if* amplifiers ($f_{if}$ ~ 4 GHz, gain 57dB) and either a square law detector or a spectrum analyzer.

For the initial circuits, the LC resonance of the SIS mixer fell outside the band of the rest of the circuitry, and the best response of the SIS mixer was obtained at about 100 and 260GHz. Weak responses at about 350 GHz were also seen in this case. The response was mapped out in a couple of slightly different geometries, and the passbands were well described by the predictions obtained from CAD modeling.

4.1 Detection of resonant soliton oscillation

When $j_c$ was less than 1 kA/cm$^2$, strong responses were observed in the SIS detector junction to radiation at around 100GHz from resonant motion of fluxons in the LJJs. Shapiro steps and photon-assisted-tunneling steps in the dc I-V curves of the SIS detectors agree with the radiation frequency given by Eq.2. An independent check of the oscillation mode can be done by changing the bias of a LJJ, from a resonant step (ZFS) in the positive branch to the negative branch. For a RSO, its radiation can be detected in both bias branches, while for an FFO, the direction of the radiation is dependent on the Lorentz force given by the vector product of the current and the magnetic field. Thus, for the FFO, the velocity-matching step is more pronounced in one branch, and so is the radiation.

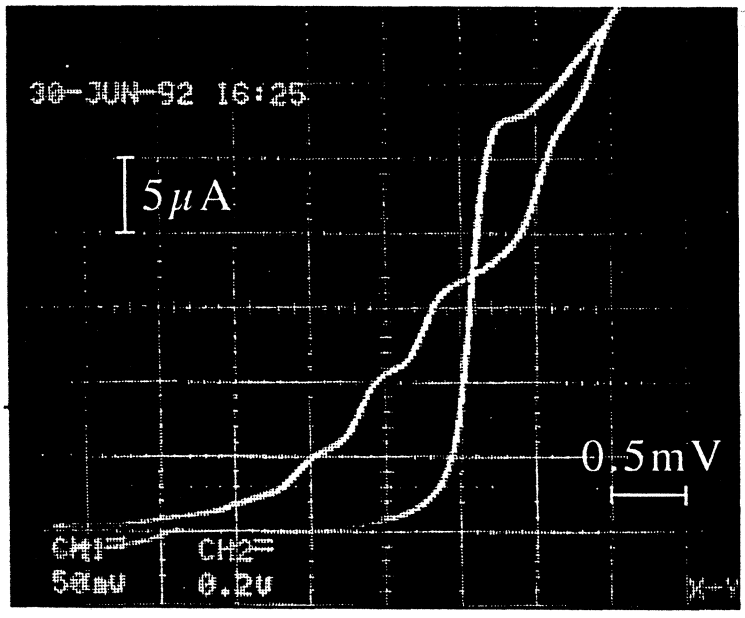


**Fig.7** Detection of radiation from a low $j_c$ RSO ($j_c$ =250 A/cm$^2$) at about 106 GHz. dc I-V curves for an SIS detector junction at 4.2 K with and without radiation. The LJJ is biased on a resonant step at $V_{osc}$ = 439.7 μV, $I_{osc}$ = 0.963 mA.

In Fig.7, we show the response of an SIS detector to the radiation from a resonant soliton oscillator that has a low $j_c$ value. When the LJJ was biased on a ZFS (~440 μV) enhanced by a weak magnetic field, clear photon assisted tunneling steps corresponding to the radiation frequency (~106 GHz) appeared in the I-V curve of the detector. We believe the radiation is from the resonant motion of multi-fluxons in a bunched configuration. In this figure, the Josephson pair current was suppressed. When the Josephson current was present, we also observed Shapiro steps in the I-V curve which corresponded to the 106 GHz radiation.

The embedding circuitry (admittance $Y_S=G_S+jB_S$ as well as the magnitude of an equivalent current source $I_S$ ) for the SIS element can be calculated from Tucker's quantum theory of mixing [22] by using the pumped and unpumped I-V curves [23].The *rf* voltage amplitude $V_{rf}$ across the SIS detector can then be calculated from

$$V_{rf} = \frac{I_S}{|Y_S + Y_{f,k}|} \quad , \qquad (10)$$

where $Y_{f,k}$ is the non-linear admittance at the bias point. The incident available power $P_{LO}$ and the absorbed power $P_{det}$ in the SIS can be calculated from

$$P_{LO} = \frac{I_S^2}{8G_S} \quad , \qquad (11a)$$

$$P_{det} = V_{rf}^2 \mathrm{Re}(Y_{f,k})/2 \quad . \qquad (11b)$$

For the I-V curves in Fig.7, we calculated $V_{rf}=0.77\,\mathrm{mV}$, $P_{LO}=4.1\,\mathrm{nW}$, and $P_{det}=3.2\,\mathrm{nW}$. For the LJJ, the current step height times the step voltage gives $0.33\,\mu\mathrm{W}$ for the LJJ. This dc-bias level fits well with the CAD modeling (i.e. about 20dB loss for this window). It also implies that the output power should be more than 20dB larger at the output end of the LJJ. For this sample, we also detected weak radiation around 106 GHz when the oscillator was biased on a resonant steps at around $\pm 220\,\mu\mathrm{V}$. This radiation could come from the second harmonic oscillation of a resonant soliton motion which has its fundamental frequency at 53 GHz.

4.2 Detection of flux-flow oscillation

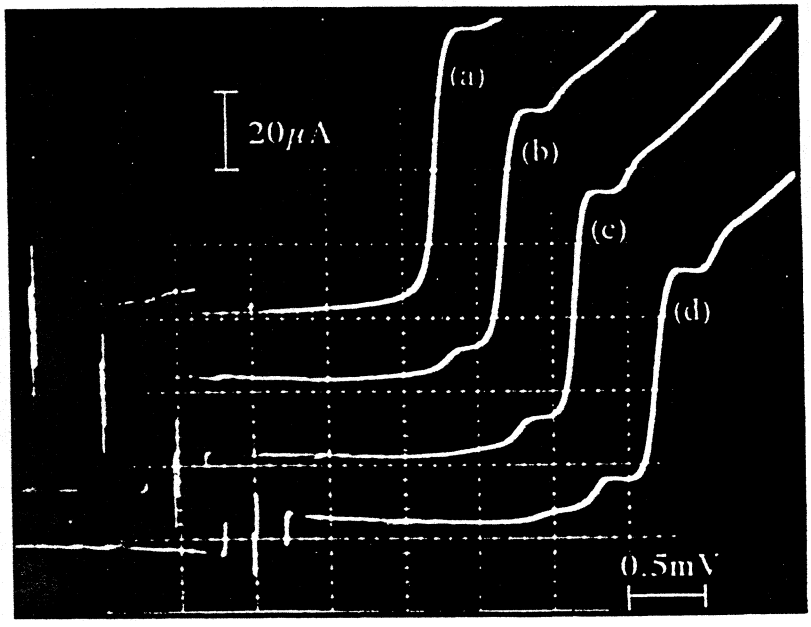


**Fig.8** Detection of radiation from an FFO at about 98GHz. The dc I-V curves for an SIS detector junction at 4.2K is shown with no radiation (a) and (b-d) for increasing LO powers. The LJJ is biased on a VM step at $V_{osc}$=202.6 μV, $I_{osc}$=1.903 mA, 1.983 mA and 2.111 mA for curves (b), (c), and (d), respectively. Negative dynamic resistance appears at the first photon induced step for enough pumping powers. This indicates that the junction capacitance is tuned out at this frequency. Shapiro steps were also obtained for large pump powers.

Measurements showed that, for LJJs which had $j_c > 1\,kA/cm^2$, VM steps due to the unidirectional flux-flow motion were easily induced and their voltages could be tuned by an external field linearly over a wide range, typically from 0.2mV (100GHz) to 1.2mV (600GHz), for our Nb/NbOx/PbBi junctions. As the voltage of a VM step was gradually increased with the field, the step height decreased and the step steepness decreased. This indicates that the output power decreases and the linewidth increases with increasing oscillator frequency. Above a certain bias close to 1.4mV, the step suddenly disappeared, which may be due to the flux flow oscillation reaching the gap frequency.

We observed radiation from the flux-flow motion at around 100GHz and 260GHz [6], and in the band 280 - 330GHz [11]. At these three frequencies, both Shapiro steps and photon-assisted tunneling were clearly seen in the SIS element. The oscillation mode was confirmed by changing the bias polarity and from Eq.3. Radiations at 350GHz, 400GHz, and 600GHz were also observed from the first Shapiro step at 0.72mV, 0.83mV, and 1.24mV, respectively.

We show in Fig.8 the response of an SIS detector ($R_n = 32.3\Omega$) to the radiation from a flux-flow oscillator with $j_c = 1.4\,kA/cm^2$. Both photon assisted tunneling steps and Shapiro steps corresponding to radiation at 98 GHz was observed. The response became more and more pronounced (Fig.8 b-d) when the oscillator's bias was moved from the bottom of the step to the top. The oscillator was biased at around 203μV. Using Eqs.(10) and (11), we obtain $V_{rf} = 0.27\,mV$, $P_{LO} = 3.7\,nW$, and $P_{det} = 2.8\,nW$. Calculations also show that the SIS mixer has a conversion gain of +2dB (for curve d in Fig.8) due to the appearance of a negative dynamic resistance at the first photon-induced step. The SIS junction area was $4\,\mu m^2$ for this sample.

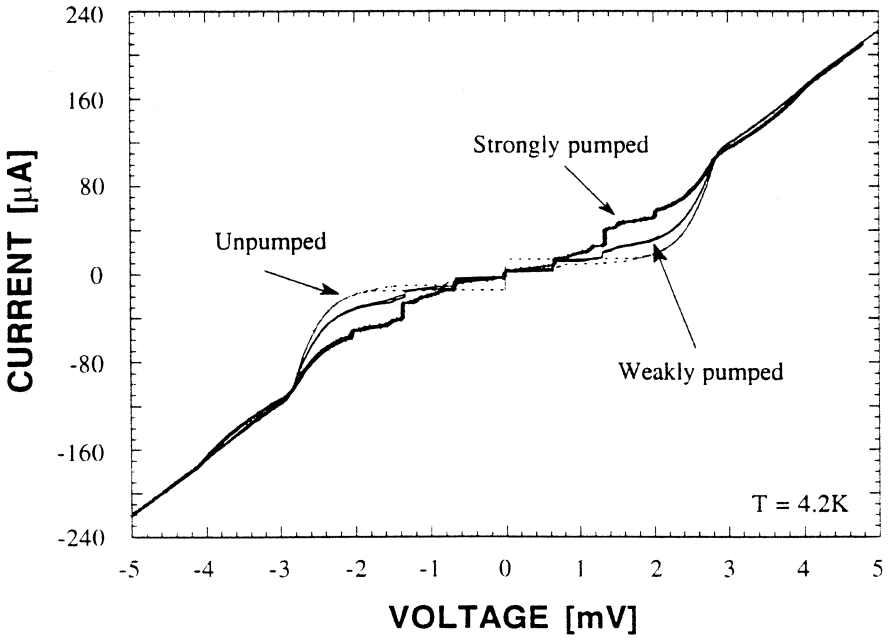


**Fig.9** Response of the SIS detector to radiation from FFO1. For the weakly pumped I-V, the FFO1 was biased at $V_{osc}$=651μV (315GHz), and the calculated available power $P_{LO}$ is 110nW. For the strongly pumped case, $V_{osc}$=663 μV (330GHz) and $P_{LO}$=430nw. The same external field was supplied in both cases.

After adjusting the area of the element and the length of the tuning strip inductance carefully, the LC resonance moved to the desired center frequency, and a good response was observed from 280 to 330GHz (580μV to 690μV) with the LC resonance at 340GHz, as shown in Fig.9. This response bandwidth (Δf=50GHz) fits well with the CAD simulation. The *rf* power from the oscillator, which could be tuned by changing the current bias along the VM step, is high enough to pump the SIS element for mixing purpose. The maximum response was at 330GHz (660μV), with a calculated power $P_{LO}=430\mu W$. This sample had quite a high $j_c$ value ~ 12kA/cm$^2$, which gave a broad detection bandwidth (around the LC resonant frequency) for the SIS element. The SIS junction had a small junction area of 0.65μm$^2$, compensated by a 13μm long strip inductance.

## 5. LINEWIDTH MEASUREMENTS OF THE FLUX-FLOW OSCILLATOR

The linewidth was determined for the flux-flow type oscillator, i.e. for the viscous unidirectional fluxon motion. Since two FFOs were mixed in an SIS element, the experimental set-up became fairly elaborate. For the dc-biasing of the FFOs and the mixer we needed 5 bias supplies - 2 for each oscillator and one for the mixer. Since the *if* amplifiers were operating at 4 GHz and had a bandwidth of about 1 GHz, the difference in voltage bias of the two oscillators had to be in the regime 7 – 10μV. First the control currents for the oscillators were adjusted to give a velocity matching (VM) step near a voltage corresponding to the band of interest. The response of the SIS mixer was monitored for each oscillator separately, and after adjusting the control currents and the oscillator biases, the amplified *if* signal was measured with a square law detector and monitored versus the voltage bias of the SIS element, as shown in Fig.10. This picture resembles the typical *if* output power versus voltage bias of the SIS mixer. However, this may not be a proof for mixing of two harmonic signals. Indeed, in some cases we found that even though the *if* output power from the SIS mixer was high and the bias dependence reasonable, the weakly coupled oscillator usually was too much off-set in bias from the strongly coupled one, and only an increased noise level with no additional structure could be seen when the spectrum analyzer was connected.

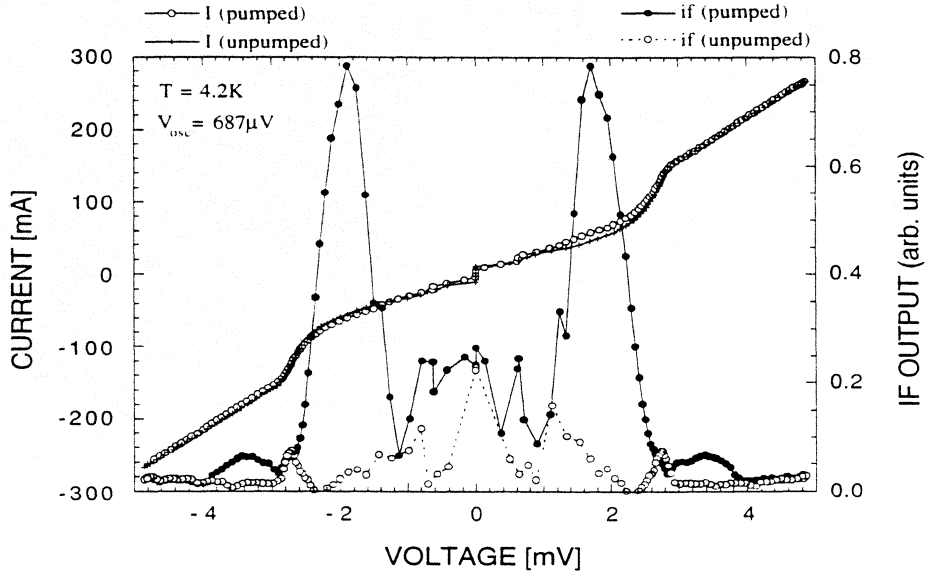


**Fig.10** dc I-V curves of the SIS mixer and the *if*-output power, with and without radiation. Both FFOs oscillate at around 330GHz.

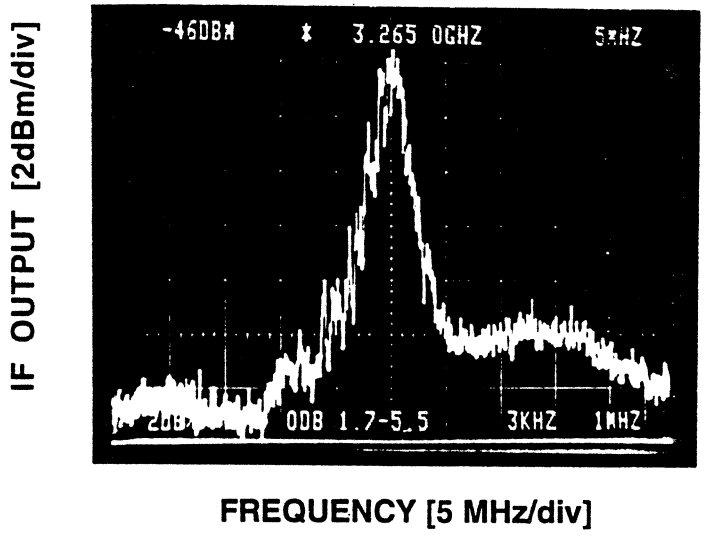


**Fig.11** Spectrum of the *if*-power at 1.4 K when the signal of FFO2 is mixed with the FFO1 (as the local oscillator) in the SIS mixer at around 320GHz. The center *if* frequency is 3.265 GHz.

After the response such as the one seen in Fig. 10 was obtained, the signal was brought to a spectrum analyzer instead. Fig.11 shows a typical recording of the *if* output, when spectral response showed mixing from coherent signals. This spectral response (with somewhat different amplitudes) was seen from 280 GHz to 330 GHz. Although, the drawback of our method is that we obtain the composite linewidth of the two oscillators, we do not have to deal with an external source of a different kind, which could add uncertainties of the upper limit of the linewidth. The composite linewidth ( - 3 dB) of the FFOs in our measurement was 2.1 MHz across this band.

## 6. CONCLUSIONS

An integrated receiver circuit was built to investigate radiation from long Josephson junctions. The radiation from two flux-flow oscillators was detected or mixed in an SIS mixer. Extensive CAD modeling of the circuit was done before the actual receiver was built. A good agreement between the experimental data and the modeling was obtained. We measured the linewidth of the flux-flow oscillators to be less than 2 MHz in the band 280-330 GHz. The frequency was tuned by changing the control current to the FFO. The output power within the same frequency interval was 0.5μW coupled to a 10Ω microstripline. The output power from the oscillator could conveniently be tuned by changing the current bias on the velocity matching step. By varying the critical current density $j_c$, we could operate the long Josephson junction both in the resonant soliton regime ($j_c < 1\text{kA/cm}^2$), and in the unidirectional flux-flow regime ($j_c > 1\text{kA/cm}^2$).

## ACKNOWLEDGEMENTS

We thank H. Zirath, I. Angelov and H. Ekström for their help, and N.F. Pederson, A.V. Ustinov and M. Cirillo for helpful discussions. The circuits were made in the Swedish Nanometer Laboratory. This work was supported by the Swedish National Board for Industrial and Technical Development (NUTEK) and the Swedish Research Council for Engineering Sciences (TFR).

## REFERENCES


[1] B. Bi, S. Han, J.E. Lukens, and K. Wan, "Distributed Josephson junction arrays as local oscillators", IEEE Trans. Appl. Supercond., MAG-27, to be published, (1993).

[2] T. Nagatsuma, K.Enpuku, K. Yoshida, and F. Irie, "Flux-flow-type Josephson oscillator for millimeter and submillimeter wave region. II. Modeling", J. Appl. Phys., 56, 3284-3293, (1984).

[3] Y.M. Zhang, "Effect of losses on the output voltage of a flux-flow type Josephson oscillator," in *Nonlinear Superconductive Electronics and Josephson Devices*, New York: Plenum Press, G. Costabile, S. Pagano, N. F. Pederson, and M. Russo, eds., (1991), pp.145-153.

[4] N.F. Pederson, "Solitons in Josephson transmission lines," in *SOLITONS*, Amsterdam: Elsevier Science Publishers B.V., S. E. Trullinger, V. E. Zakharov, and V. L. Pokrovsky, eds., (1986), pp.469-501.

[5] E. Joergensen, V.P. Koshelets, R. Monaco, J. Mygind, M.R. Samuelsen, and M. Salerno, "Thermal fluctuations in resonant motion of fluxons on a Josephson transmission line: Theory and Experiment", Phys. Rev. Lett., 49, 1093-1096, (1982).

[6] Y.M. Zhang, D. Winkler, and T. Claeson, "Detection of mm and submm wave radiation from soliton and flux-flow modes in a long Josephson junction", IEEE Trans. Appl. Supercond., MAG-27, to be published, (1993).

[7] M. Cirillo, F. Santucci, P. Carelli, M.G. Castellano, and R. Leoni, "Coupling of long Josephson junction oscillators at millimeter-wave frequencies", IEEE Trans. Appl. Supercond., MAG-27, to be published, (1993).

[8] T. Nagatsuma, K. Enpuku, F. Irie, and K. Yoshida, "Flux-flow-type Josephson oscillator for millimeter and submillimeter wave region", J. Appl. Phys., 54, 3302-3309, (1983).

[9] T. Nagatsuma, K. Enpuku, K. Sueoka, K. Yoshida, and F. Irie, "Flux-flow-type Josephson oscillator for millimeter and submillimeter wave region. III.Oscillation stability", J. Appl. Phys, 58, 441-449, (1985).

[10] Y.M. Zhang and P.H. Wu, "Numerical calculation of the height of velocity-matching step of flux-flow type Josephson oscillator", J. Appl. Phys, 68, 4703-4109, (1990).

[11] Y.M. Zhang, D. Winkler, and T. Claeson, "Linewidth measurements of Josephson flux-flow oscillators in the band 280-330 GHz", Appl. Phys. Lett., to be published, (1993).

[12] A.V. Ustinov, T. Doderer, R.P. Huebener, J. Mygind, V.A. Oboznov, and N.F. Pedersen, "Multi-fluxon effects in long Josephson junctions", IEEE Trans Appl. Supercond., MAG-27, to be published, (1993).

[13] V.P. Koshelets, A.V. Shchukin, S.V. Shitov, and L.V. Filippenko, "Superconducting millimeter wave oscillators and SIS mixer integrated on a chip", IEEE Trans. Appl. Supercond., MAG-27, to be published, (1993).

[14] H.A. Atwater, "Microstrip reactive circuit elements", IEEE Trans on Microwave Theory and Technology, MTT-31, 488-491, (1983).

[15] A.R. Kerr and S. Pan, "Some recent developments in the design of SIS Mixers," in *First Int. Symp. on Space Terahertz Technology*, Michigan, (1990), pp.363-377.

[16] R. Blundell and D. Winkler, "The superconductor-insulator-superconductor mixer receiver - a review," in *Nonlinear Superconductive Electronics and Josephson Devices*, New York: Plenum Press, G. Costabile, S. Pagano, N. F. Pedersen, and M. Russo, eds., (1991), pp.55-72.

[17] W.H. Chang, "The inductance of a superconducting strip transmission line", J. Appl. Phys., 50, 8129-8134, (1979).

[18] W.H. Chang, "Measurement and calculation of Josephson junction device inductances", J. Appl. Phys., 52, 1417-1426, (1981).

[19] W.H. Henkels and C.J. Kircher, "Penetration depth measurements of type II superconducting films", IEEE Trans. on Magn., MAG-13, 63-66, (1977).

[20] H.K. Olsson, "Dielectric constant of evaporated SiO at frequency between 13 and 103GHz", IEEE Trans. Magn., MAG-25, 1115-1118, (1989).

[21] R.E. Collin, *Foundations for microwave engineering*, Tokyo: McGraw-Hill, 1966, Chapter 5.

[22] J.R. Tucker and M.J. Feldman, "Quantum detection at millimeter wavelengths", Rev. Mod. Phys., 57, 1055-1113, (1985).

[23] A. Skalare, *SIS Embedding Circuit Program for Macintosh*, Version 2.5, 1993.